Self-assembled hybrid precursors towards $NiMoO_4$ more efficient propane ODH catalysts

B. Farin[1], P. Eloy[2], C. Poleunis[2], M. Devillers[1] and E.M. Gaigneaux[1]**

[1] *Institute of Condensed Matter and Nanoscience - MOlecules, Solids and reactiviTy (IMCN / MOST).Université catholique de Louvain. Croix du Sud 2 box L7.05.17, 1348 Louvain-La-Neuve, Belgium*

[2] *Institute of Condensed Matter and Nanosciences - Bio-and Soft Matter (IMCN / BSMA), Surface Characterisation Platform (SUCH), Université catholique de Louvain, Croix du Sud 1/L7.04.01, 1348 Louvain-la-Neuve, Belgium*

*Corresponding authors: michel.devillers@uclouvain.be, eric.gaigneaux@uclouvain.be

Supplementary information

Detailed XPS experimental

X-ray photoelectron spectroscopy (XPS) was performed on a Kratos Axis Ultra spectrometer (Kratos Analytical) equipped with a monochromatized aluminum X-ray source powered at 10 mA and 15 kV. The powder samples were gently pressed with a spatula on an isolating double sided adhesive tape fixed on a polyacetal polymer piece. The pressure in the analysis chamber was about 10^{-6} Pa. The angle between the normal to the sample surface and the direction of photoelectron collection was 0°. Analyses were performed in the hybrid lens mode which is a combination of magnetic and electrostatic lenses. The slot aperture was used, the iris drive position was set at 0.5 and the analyzed area was 700 µm x 300 µm. The pass energy of the hemispherical analyzer was set at 160 and 40 eV for the survey scan and the narrow scans respectively. In such conditions, the full width at half maximum (FWHM) of the $Ag_{3d5/2}$ peak of a standard silver sample was about 0.9 eV. The charge stabilization was achieved by means of an electron source co-axially mounted to the electrostatic lens column. A charge balance plate (-4 V) was used to reflect electrons back towards the sample. The magnetic field of the immersion lens placed below the sample acted as a guide path for the low energy electrons returning to the sample. The electron source was operated under a filament current of 0.16 A and a bias of -1.2 eV.

The following sequence of spectra was recorded: survey spectrum, C_{1s}, O_{1s}, N_{1s}, Ni_{2p}, Cl_{2p} and C_{1s} again. The latter allowed checking the charge stability as a function of time and the absence of sample degradation during the analyses. The C-(C,H) component of the carbon C_{1s} peak was fixed at 284.8 eV to set the binding energy scale. The spectra were decomposed with the CasaXPS program (Casa Software Ltd.) with a Gaussian/Lorentzian (70/30) function product and after the subtraction of a linear baseline. The shape of different Ni references was used for the decomposition of the Ni_{2p} doublet. Molar fractions (%) were calculated by using peak areas normalized on the basis of acquisition parameters, the subtraction of a linear background, experimental sensitivity factors and transmission factors provided by the manufacturer. Element molar fractions were provided, excluding hydrogen which is not detected by XPS.

TGA data

Table S1: Water fraction measured at 150°C of the C12 matrix, the ions alone and hybrid materials containing Ni & Mo ions. The water fraction trapped within the C12 matrix and the one linked to the insertion of ions were also calculated in the third and fourth column respectively.

Material	Measured water fraction (% wt.)	C12 matrix water fraction (% wt.)	Water fraction increase (% wt.)
C12 matrix	4.9	4.9	0.0
I/R ratio = 0.25	6.3	4.1	2.2
I/R ratio = 0.5	6.4	3.6	2.8
I/R ratio = 1	6.5	2.9	3.6
I/R ratio = 1.5	6.7	2.4	4.3
I/R ratio = 2	6.2	2.1	4.1
I/R ratio = 3	7.3	1.6	5.7
I/R ratio = 4	7.6	1.3	6.3
Ions alone	9.6	-	-

The general Ni – COO^- coordination modes

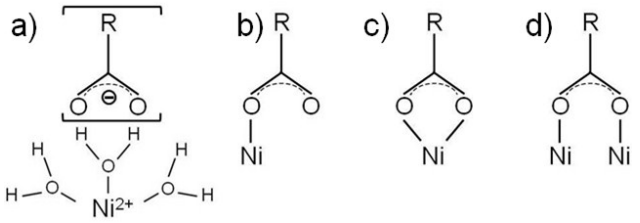

Scheme S1: General modes of the Ni – COO^- coordination: the electrostatic mode (a), the monodentate coordination (b), the bidentate chelate coordination (c) and the bidentate bridging coordination (d) (schemes redrawn from Strathmann et al. work [20]).

XRD data of the hybrids containing Ni ions or Mo ions only

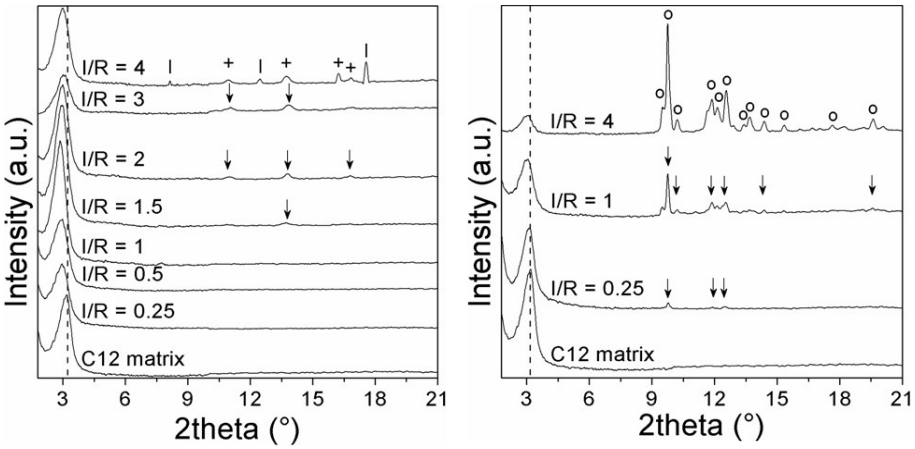

Figure S1: Diffractograms of hybrid materials containing Ni ions only (left) and Mo ions only (right). Three crystalline phases were identified: $Ni(NO_3)_2.6H_2O$ (I), $Ni_2(NO_3)_2(OH)_2.2H_2O$ (+) and $(NH_4)_6Mo_7O_{24}.4H_2O$ (°).

XRD data on the catalysts obtained by calcination of the hybrids

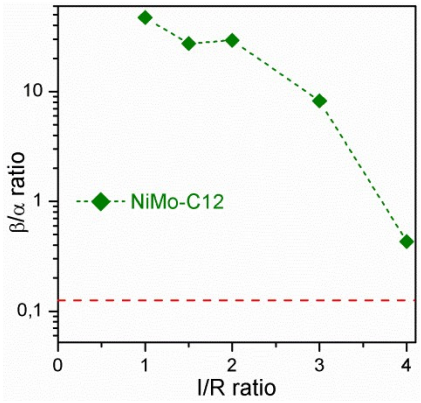

Figure S2: Evolution of the β/α ratio of $NiMoO_4$ as a function of the amount of Ni – Mo ions (I/R ratios: 1 - 4) added to the C12 matrix. These oxides were produced by calcination at 500 °C for 4 h. The horizontal dashed red line represent the β/α ratio of a co-precipitated $NiMoO_4$.

Oxidation state of Ni and Mo at the surface of the nickel molybdates synthesized in this work.

Table S2: Binding energies (BE) measured by XPS of the $Mo3d_{5/2}$ and $Ni2p_{3/2}$ peaks of the $NiMoO_4$ made from the co-precipitation and hybrid precursor methods.

Calcined Material	BE of $Mo3d_{5/2}$		BE of $Ni2p_{3/2}$
NiMo-Cop	232.5 ± 0.2 eV		855.7 ± 0.2 eV
NiMo-C12 I/R = 1	232.6 ± 0.2 eV		856.1 ± 0.2 eV
$NiMoO_4$ from ref [9]*	232.6 ± 0.2 eV		855.7 ± 0.2 eV

*L. M. Madeira, M. F. Portela and C. Mazzocchia, *Catalysis Reviews-Science and Engineering*, 2004, **46**, 53-110.

The oxidation state of Ni and Mo in the synthesized nickel molybdates can be deduced from the data presented in this table S2. The first thing that can be observed is that the recorded data are in line with the literature. Other authors obtained similar BE values with the nickel molybdate system. According to this literature, Mo in our catalysts likely exists in the most oxidized Mo6+ state as the recorded values are quite close the BE of the $Mo3d_{5/2}$ peak of MoO_3 [9]. Regarding Ni, the situation stays less clear due to the complexity of the XPS Ni2p region. Ni in our catalysts likely exists in an oxidized state as the binding energy remains far higher to the BE range of metallic nickel (854 eV and lower). However, evidencing the oxidation state more precisely is difficult as the position of the peak depends on the oxidation state but also on the crystalline phase and the nature of the atoms surrounding Ni (here O and Mo). Despite this, we can underline that the BE of the $Ni2p_{3/2}$ peak of our catalysts is in the similar range observed in the literature. This suggests that nothing that was unexpected happened to our catalyst. Moreover, XRD results showed the highly crystallized state of our catalysts. Both α- and β-$NiMoO_4$ were indeed detected where Ni is known to exist in the 2+ state. This is why Ni likely exists in our samples in the 2+ state. So, in conclusion, we can state that Mo and Ni both tend to exist in our catalysts in an oxidized state namely 6+ and 2+. Such a conclusion appears quite logic as (i) the catalysts were obtained by the calcination of the hybrids for a long time period (4h) under air namely an ambiance being rich in oxygen, and (ii) the hybrids were constituted from salts where Ni and Mo were already in the 2+ and 6+ states.

Catalyst stability over time

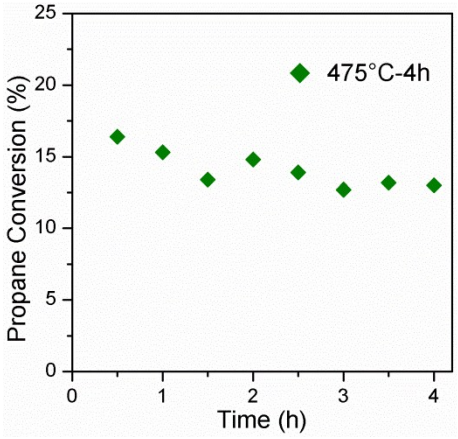

Figure S3: Propane conversion of the NiMo-C12 I/R=1 catalyst over time. The catalyst has been calcined at 475°C.